

Modeling and Optimization of Oil Adsorption from Wastewater Using an Amorphous Carbon Thin Film Fabricated from Wood Sawdust Waste Modified with Palmitic Acid

Sherif A. Younis^{1,2} · Mona El-Sayed^{1,2} ·
Yasser M. Moustafa^{1,2}

Received: 13 September 2016 / Accepted: 8 December 2016 / Published online: 24 December 2016
© Springer International Publishing Switzerland 2016

Abstract Economic, reusable and renewable adsorbents are prepared by surface functionalization of wood sawdust (WD) based amorphous carbon thin film (ACTF) using long-chain palmitic fatty acid (PAC). The prepared adsorbents were characterized by FTIR, HR-TEM, SEM, and N₂ physisorption (BET) techniques. The WD-PAC and ACTF-PAC materials reflect a good gasoline and condensate oil adsorption capacity (q_e , mg.g⁻¹) from wastewater with high kinetics rates within 2–4 h contact time. Kinetic adsorption was found to behave as a pseudo-second kinetic model and controlled by a diffusion mechanism with an exothermic nature. The initial oil adsorption rates, h_0 (mg.g⁻¹.h⁻¹) for gasoline and condensate oil were 72.5–109.9 mg.g⁻¹.h⁻¹ and 322.6–384.6 mg.g⁻¹.h⁻¹, respectively, by WD-PAC and ACTF-PAC. Equilibrium data reflected favorable fit with multiple Langmuir-Freundlich isotherm model and the maximum monolayer $q_{e,calc}$ (mg.g⁻¹) was calculated respectively as 363.3 and 447.4 mg.g⁻¹ for condensate oil using WD-PAC and ACTF-PAC. Response surface methodology (RSM) was successfully utilized to optimize and simulate four statistical quadratic polynomial models to predict the oil uptake by the prepared adsorbents. The quality of the models was judged by analysis of variance (ANOVA) at 95% confidence limit ($p < 0.05$). The quadratic interaction effects between adsorbent dose (2.5–7.5 g.L⁻¹) and initial oil concentrations (0.1–2.5 g.L⁻¹) by ACTF-PAC shows no significant effect (p -value of 0.198 and 0.687), indicating the improvement of the hydrophobic surface characteristics after

Electronic supplementary material The online version of this article (doi:10.1007/s40710-016-0202-y) contains supplementary material, which is available to authorized users.

✉ Sherif A. Younis
sherifali_r@yahoo.com; sherifali@epri.sci.eg

¹ Analysis and Evaluation Department, Egyptian Petroleum Research Institute, 11727 Nasr City, Cairo, Egypt

² Water Unit, Central Laboratories, Egyptian Petroleum Research Institute, 11727 Nasr City, Cairo, Egypt

functionalization. In addition, the WD-PAC and ACTF-PAC adsorbents proved to be a potential candidate for oil contamination prevention and/or recovery even after ten cycles.

Keywords Superhydrophobic amorphous carbon thin film · Oil pollution treatment · Adsorption-desorption study · Kinetic and isotherm modeling · Adsorption mechanism · Response surface optimization

1 Introduction

With the increase of petroleum industries and oil production and the frequent oil-spill accidents, there is a growing demand for developing effective materials able to remove oil contaminants from water environments (Ge et al. 2014; Fard et al. 2016). The oily wastewater treatment is important not only from an economic viewpoint, but also to end water resources contamination (Xiaobing et al. 2010). Over the past decades, various technologies such as physical, chemical, de-emulsifying, advanced oxidation, biological and electrochemical treatments have been developed for treating oil and organic contaminated wastewater (Dong et al. 2011; Roustaei et al. 2013; Chen et al. 2014; Roberts and Inniss 2014; Hosny et al. 2016). The adsorption process, however, is one of the effective techniques not only for oil removal and wastewater treatment but also for adsorbate recovery under ambient conditions (Ibrahim et al. 2010; Okiel et al. 2011; Fard et al. 2016; Jain and Malik 2016; Pan et al. 2016; Wang et al. 2016). Activated carbon (AC) is generally the most widely used adsorbent for eliminating oil from wastewater because of its extended surface area, microporous structure, high adsorption capacity, and high surface reactivity (Nuithitikul et al. 2010; Hartmann et al. 2014; Raj and Joy 2015). However, commercial AC is expensive and might not be economic for heavy oily wastewater treatment. Therefore, development of high efficient AC thin film (ACTF) from locally zero-cost wood sawdust (WD) wastes is an interesting option for an economic industrial wastewater treatment. WD is one of the major zero-cost waste materials that is abundantly available in furniture, timber and paper industries (Cambiella et al. 2006; Meniai 2012; Heibati et al. 2015). Thus, WD, as a precursor of ACTF, will give a value-added product from a low-cost material.

In recent years, fabrication of superhydrophobic materials has found their spectacular advantages such as oil recovery, anti-corrosion, water repellency, self-cleaning, anti-sticking and so forth (Zang et al. 2015). In theory, superhydrophobic terms should be the incorporation of micro–nano rough surface structure with low surface free energy (Zang et al. 2015; Gupta et al. 2016). Because of its outstanding characteristics, various approaches have been developed for the acquisition of superhydrophobic adsorbent surface involving layer-by-layer assembly, solution-immersion process, chemical etching, steam impingement, ultrasound irradiation and others (Banerjee et al. 2006; Ge et al. 2014; Zang et al. 2015). But, using less expensive long chain fatty acids as the modifying agent is still rare. Hence, the functionalization of WD and ACTF with palmitic fatty acid to obtain low-cost, chemical durability, and efficient superhydrophobic adsorbent surface through a simple drop-coating method would show better performance in heavy oil wastewater treatment.

The present study aims to enhance the heavy oils (such as Egyptian gasoline and condensate oil) adsorption from wastewater systems by superhydrophobic amorphous carbon thin film (ACTF) based wood sawdust (WD). Adsorbent surface functionalization by palmitic fatty acid (PAC) was utilized to increase superhydrophobic characteristics and enhance oil removal.

The experimental oil adsorption data were studied for some of theoretical kinetic, isotherm and thermodynamic models to elucidate the mechanism involved in the oil adsorption. In addition, the main and interaction influential effect of experimental variables such as adsorbent dose, initial oil concentrations, and temperature on oil adsorption responses was investigated through response surface cubic plots. Response surface methodology (RSM) combined with multiple regression analysis techniques was utilized for optimization of oil adsorption and development of the empirical models correlating the adsorption responses.

2 Experimental Methods

2.1 Preparation of Superhydrophobic Amorphous Carbon Thin Film Adsorbent

Mixed wood sawdust (WD) wastes collected from local workshop furniture trade in Egypt was crushed and sieved to a mesh size of 0.1–0.07 mm. The crushed WD was washed with hot deionized water and dried in a hot air oven at 333 K to a constant weight. Then, 50 g dried WD was treated by concentrated sulfuric acid in a 500 mL quartz reactor and vigorously stirred for 30 min in the presence of 1 g active silica. The obtained matrix was filtered and washed with hot deionized water until near neutral pH (6–7), then oven dried and semi-carbonization took place using a microwave oven set at 450 Watt for 20 min. Later, the semi-carbonized product was mixed with 0.01 g cobalt silicate nanoparticles and heated up to 323 K for 30 min. The resultant amorphous carbon thin film (ACTF) was left to cool, then washed and vacuum dried at 333 K for 24 h, and then stored in a desiccator until used.

Palmitic fatty acid (PAC, Sigma Aldrich, St. Louis, MO, USA) grafted adsorbents (WD-PAC and ACTF-PAC) were prepared as herein after. In three-necked glass reactors equipped with mechanical stirrer, reflux condenser and thermometer, 10 g of dried WD or ACTF in 100 mL of n-hexane were refluxed with 15 mol PAC for 6 h under nitrogen atmosphere. After that, the esterified adsorbent (WD-PAC or ACTF-PAC) was washed repeatedly with n-hexane, then vacuum dried at 338 K for 24 h and stored until used.

2.2 Characterization

The surface functional groups of the prepared adsorbents were analyzed by Fourier-transform infrared (FTIR) instrument model spectrum one (Perkin Elmer, USA). Scanning electron microscope (SEM, JEOL JSM 6710 F, Japan) and high resolution transmission electron microscope (HR-TEM, model JEOL JEM 2200FS at 200 kV) were used to examine the surface morphology microstructure before and after adsorption. The surface areas of the prepared adsorbents were determined using Nov. 3200 Autosorb analyzer (Quantachrome, USA).

2.3 Batch Adsorption of Oil and RSM Statistical Optimization

The oil–water mixture of Egyptian condensate and gasoline oil was prepared at the desired concentration using synthetic wastewater as described by Younis et al. (2014). Batch adsorption experiments were conducted at 308 K by agitating 0.1 g of adsorbent with 25 mL of

1000 mg.L⁻¹ oil–water mixture in a stoppered glass Erlenmeyer flask at 150 rpm shaking speed for 24 h. The residual oil concentrations were determined based on ASTM D7678-11 (2011) and described by Yang (2011). In brief, a known volume of oil–water sample was collected after each experimental run, acidified to pH 2, and transferred to liquid funnel containing n-hexane/cyclohexane extracting solvent. The organic layer was drained over anhydrous Na₂SO₄, collected in distillation flask, and the solvent was evaporated using a rotary evaporator at 358 K until constant weight was obtained, and then the amount of oil residuals was calculated. For comparison at low detection limits <10 mg.L⁻¹, the same procedure was used with trichlorotrifluoroethane as extraction solvent, and the amount of oil extracted was measured using FTIR instrument at maximum absorbance peak of 2930 cm⁻¹ versus standard oil mixtures.

At time *t*, oil removal percentage (%) and oil uptake (*q_t*, mg.g⁻¹) were calculated by the following mass-balance equations:

$$\text{Removal\%} = \frac{(C_o - C_t)}{C_o} 100 \quad (1)$$

$$\text{Adsorption uptake } q_t = \frac{(C_o - C_t)V}{M} \quad (2)$$

where *C_o* and *C_t* are the initial and final concentrations of the oil in the mixture (mg.L⁻¹). *V* (L) is the volume of the mixture and *M* (g) is the mass of the adsorbent used. All data listed are the arithmetic average of triplicate experiments to check reproducibility with a standard deviation of ±1.25% to ±2.4% for condensate and gasoline, respectively at 95% confidence level.

2.4 Response Surface Optimization and Error Analysis

A statistically three-level CCD design space matrix formulated by RSM (Demim et al. 2013) was used to determine the optimum operating parameters such as adsorbent dose (2.5–7 g.L⁻¹), initial oil concentrations (*C_o* =100–2500 mg.L⁻¹) and temperature (288–318 K) on the adsorption of oil removal responses. Four replicates in the central point were performed to estimate the pure error (Supplementary data: Table S1) through the Design Expert® 8.0.7.1 (State-Ease Inc., Minneapolis, USA) software. The correlations between the independent variables (*x*) and oil adsorption response (*Y*, removal%) were calculated by the quadratic polynomial model (Eq. 3) to simulate the experimental data:

$$Y = \beta_o + \sum_{i=1}^3 \beta_i x_i + \left(\sum_{i=1}^3 \beta_{ii} x_i \right)^2 + \sum_{i=1}^2 \sum_{j=i+1}^3 \beta_{ij} x_i x_j \quad (3)$$

where *x_i* and *x_j* are the independent variables, *β_o*, is the constant model coefficient, *β_i*, *β_{ii}*, and *β_{ij}* are the interaction coefficients of linear, quadratic, and second-order terms, respectively. Analysis of variance (ANOVA) and the normalized standard deviation,

$\Delta q_t\%$, (Hameed 2007) were used for the statistical evaluation of how well the experimental data fit each studied model:

$$\Delta q_t\% = \frac{\sum_{i=1}^N \left| \frac{q_{t,exp} - q_{t,calc}}{q_{t,exp}} \right|}{N-1} \times 100 \quad (4)$$

where N is the number of data points, and $q_{t,exp}$ and $q_{t,calc}$ are the experimental and calculated adsorption capacities ($\text{mg}\cdot\text{g}^{-1}$), respectively.

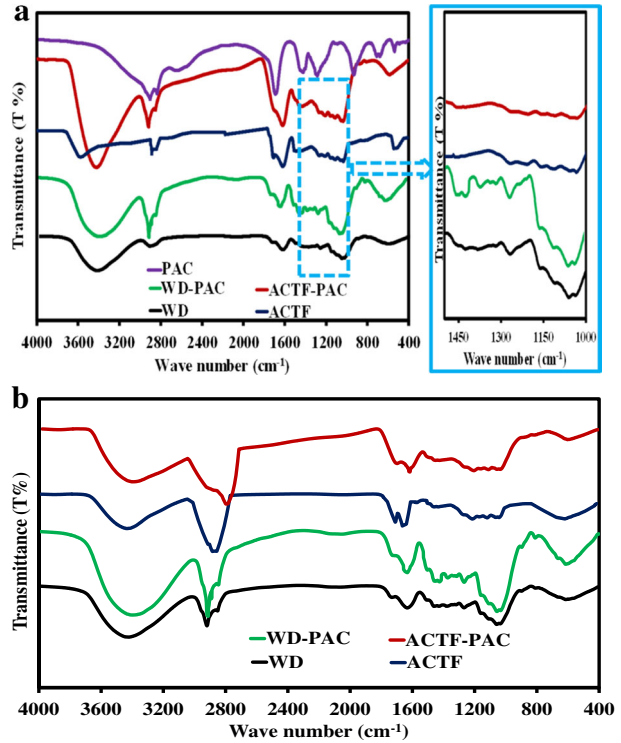
3 Results and Discussion

3.1 Characterization of the Adsorbents

The identification of the chemical structure of the four adsorbents before and after modification as well as after oil adsorption could verify the possible functional groups involved in adsorption. Figure 1 shows the FTIR spectra of WD, ACTF, WD-PAC and ACTF-PAC studied adsorbents. A strong broad band at $3650\text{--}3445\text{ cm}^{-1}$ is observed in all the prepared samples (Fig. 1), which is assigned to the intra- and inter-molecular hydrogen stretching of hydroxyl groups (Yang et al. 2007). The broad peaks at 1110 , 1060 and 1035 cm^{-1} show the C-O-C twist bending vibration of lignin and the C-O is stretching of cellulose and hemicelluloses in WD and WD-PAC (Pandey and Pitman 2003), which disappear in ACTF and ACTF-PAC (Fig. 1a). The band increase at $1730\text{--}1705\text{ cm}^{-1}$ (C=O) and $1000\text{--}1300\text{ cm}^{-1}$ (C-O) may be attributed to stretching ester linkage between the carboxyl group of PAC and WD and ACTF acid surface groups (Fig. 1a). Furthermore, the two bands at 2920 and 2850 cm^{-1} were ascribed to asymmetric and symmetric stretching of methylene C-H originated in the alkyl chains (CH_3 and CH_2) of modified WD-PAC and ACTF-PAC sorbents (Majdan et al. 2005). Resultant FTIR bands suggest the successful impregnation of PAC on to the ACTF and WD surfaces. In Fig. 1b, the increasing band at $1650\text{--}1505\text{ cm}^{-1}$ may be attributed to the C=C stretching vibration mode of olefinic oil groups. Vibration bands at $1460\text{--}1450\text{ cm}^{-1}$ and $1420\text{--}1400\text{ cm}^{-1}$ represent CH_3 and CH_2 asymmetric deformation, whilst the low intensity at $1380\text{--}1375\text{ cm}^{-1}$ corresponds to CH_3 symmetric deformation resultant from oil adsorption (Yang et al. 2007).

In Fig. 2a, the HR-TEM and its corresponding selected area electron diffraction (SAED) pattern shows that the ACTF displayed a platelet-like morphology in the form of thin films with a two-dimensional graphene sheet structure. Following PAC surface modified ACTF (ACTF-PAC; Fig. 2b), the surface has become more compacted as it is covered with a series of the hydrophobic PAC long-aliphatic chains. This reveals that the ACTF consists of multiple accumulated sheets, and, hence, in future research, the simultaneous effects of the synthetic parameters to control the thin film sheet numbers of the ACTF will be investigated for giving superiority for higher oil adsorption results. The SEM surface morphology of the prepared adsorbents is shown in Fig. 3, which indicates the changes occurring in the surface microstructures after PAC modification and oil adsorption. SEM image of WD (Fig. 3a) shows ordered structure of polysaccharides (hemicellulose-cellulose-lignin) matrix cross-interconnected pores that have corroded and become coarse in a highly porous texture after

Fig. 1 FTIR spectra of the WD, WD-PAC, ACTF and ACTF-PAC adsorbents before (a) and after (b) oil adsorption

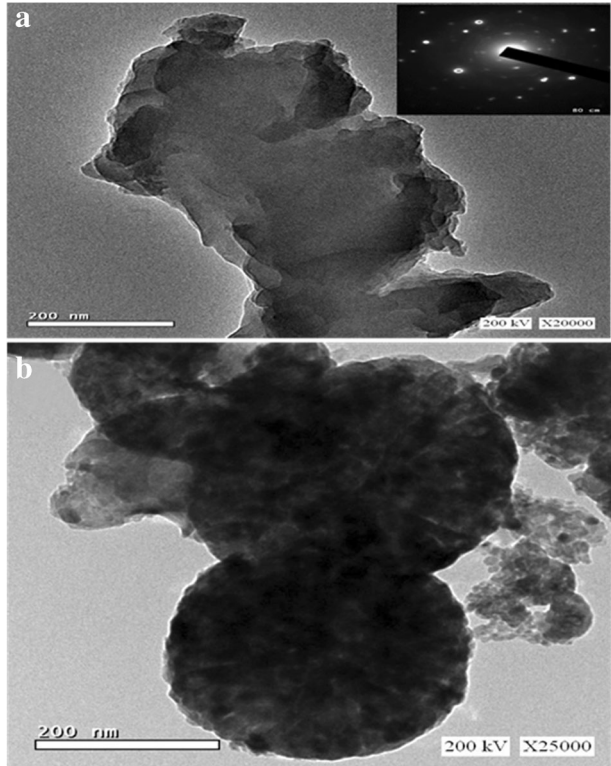


modification with PAC (WD-PAC; Fig. 3b). Figure 3c showed a corroded and disordered structure of ACTF surface texture with irregular long ridges resembling a series of parallel straight tubes which disappeared after modification with PAC (ACTF-PAC; Fig. 3d). After oil adsorption, the SEM image of ACTF-PAC (Fig. 3e) reveals that the surface is covered with a series of oil cavities and completely adhered with the adsorbent surface. Such results implied the good adsorption capabilities of oil on the prepared superhydrophobic ACTF-PAC adsorbents (Malik et al. 2004; Sidik et al. 2012; El-Sayed et al. 2016). Moreover, the BET surface areas of the studied adsorbents were recorded 18.7, 29.8, 570.1, and 650.2 $\text{m}^2 \cdot \text{g}^{-1}$ for WD, WD-PAC, ACTF, and ACTF-PAC, respectively. Such increase in the BET surface area could be related to the long chain of functional PAC aliphatic (C_{16}) hydrocarbons fatty acid. The increased BET surface area for WD-PAC and ACTF-PAC further confirmed the successful impregnation of PAC onto the WD and ACTF materials surfaces. Characterization results above suggested that the WD-PAC and ACTF-PAC could enhance the ability of oil trapping during adsorption due to the increase of the contact area and presence of free C_{16} superhydrophobic aliphatic chain on their surface (Sidik et al. 2012).

3.2 Kinetic Modeling and Adsorption Mechanism

Figure 4 graphs show that gasoline and condensate oils adsorption curves were continuous and increased directly within the first 2 to 4 h, respectively (rapid satge) using PAC grafted adsorbents, and thereafter slower with time until a constant maximum equilibrium values of

Fig. 2 HR-TEM image of the fabricated **a** ACTF and **b** ACTF-PAC adsorbents



adsorption was attained (equilibrium stage). Compared to the other adsorbent, longer contact times ranging from 8 to 10 h were required to complete the first rapid oil adsorption stage. This phenomenon indicates the improvement of the organophilic WD-PAC and ACTF-PAC to uptake the oil molecules compared to nonmodified adsorbents. From the FTIR analysis (cf. Section 3.1), it can be revealed that the PAC grafted adsorbents (WD & ACTF) reaction was done through esterification mechanism as shown in Fig. 5.

In the fabricated ester bond, both the carbon and the two oxygen atoms have sp^2 hybridization with two unshared pairs of electrons on both oxygen molecules, making it possible to have one or more π -orbital “vacant” for participation in the oil adsorption through π - π bonding mechanism, just like $C=C$. Hence, the improved adsorption affinity of WD-PAC and ACTF-PAC may be attributed to increasing the number of vacant π -orbital due to that ester-forming palmitic acid (Patai 1966; Smith and March 2007) in addition to the C_{16} -palmitic hydrophobic tails, which interact with each other producing a hydrophobic–oleophilic surface phase. This superhydrophobic phase acts as the partition medium for enhancing the retention of non-ionic organic oil components from wastewater into the functional surface sites of the PAC grafted adsorbents (Banerjee et al. 2006). When saturation of the adsorbed oil was reached at the exterior oleophilic C_{16} functional surface, the oil molecules diffused from the boundary layer film onto the exterior surface, and then entered the porous structure and then was adsorbed by the interior adsorbent surface. Regarding the experimental q_e , $mg.g^{-1}$, of oil adsorbed, the studied adsorbents can rank in the order of ACTF-PAC > ACTF > WD-PAC > WD, confirming the improvement of the organophilic degree of the prepared ACTF-PAC in

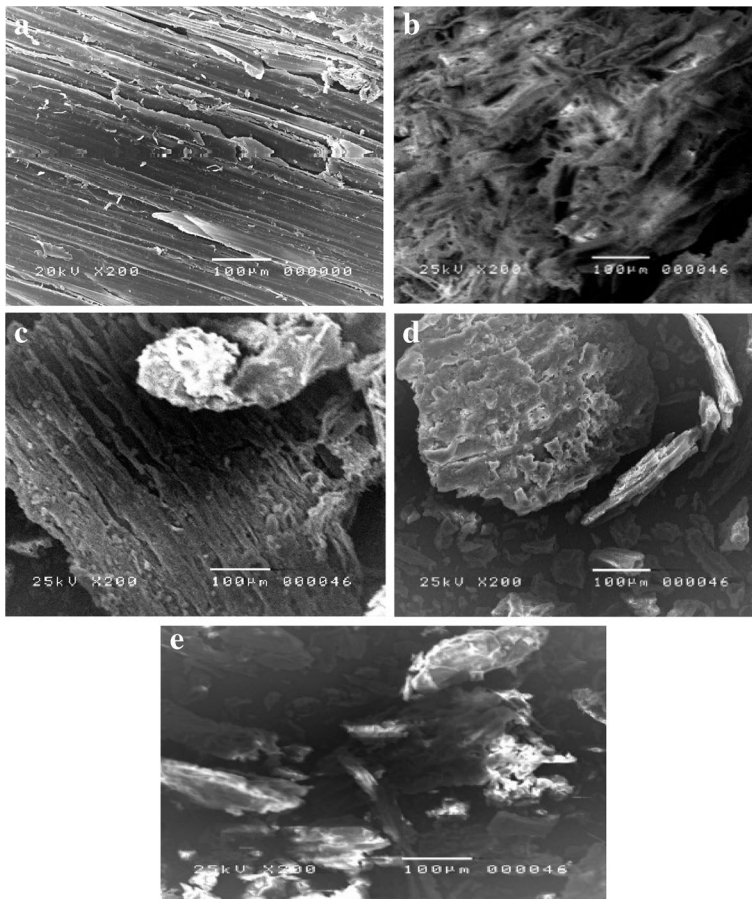


Fig. 3 SEM images for the studied adsorbents; **a** WD, **b** WD-PAC, **c** ACTF, and **d** & **e** ACTF-PAC before and after adsorption

this study. Based on the distribution coefficient (K_d) term values (Sayed and Zayed 2006; Munthali et al. 2015) and the experimental q_e , $\text{mg}\cdot\text{g}^{-1}$, for the adsorbed oil, it can be revealed that the ACTF-PAC adsorbent has a significant selectivity towards adsorption of condensate oil compared to gasoline oil with K_d values of 589.6 and 481.3 $\text{mL}\cdot\text{g}^{-1}$, and q_e values of 148.0 and 141.3 $\text{mg}\cdot\text{g}^{-1}$, respectively. The high condensate q_e results may be attributed to the higher condensate viscosity of $0.766 \text{ mm}^2\cdot\text{s}^{-1}$ compared to $0.692 \text{ mm}^2\cdot\text{s}^{-1}$ of gasoline oil based on ASTM D 445–15. This result suggests that with the increasing oil viscosity, more time is taken by oils to be deposited on the external adsorbent surface. This improves the oil adhesion property and the subsequent higher partitioning of the insoluble oil components from wastewater to the hydrophobic/oleophilic adsorbent surface phase. In this hypothesis, with the increasing oil viscosity and the oleophilic characteristic of the adsorbent surface, the rate of oil component penetration into the capillary and interior pores of the adsorbents increases, which causes high condensate oil adsorption capacity (Wu et al. 2012; Wang et al. 2013).

The kinetics of oil uptake rates were studied to examine the controlling mass transfer, and physical and chemical reaction mechanisms of adsorption. In this study, four kinetic models,

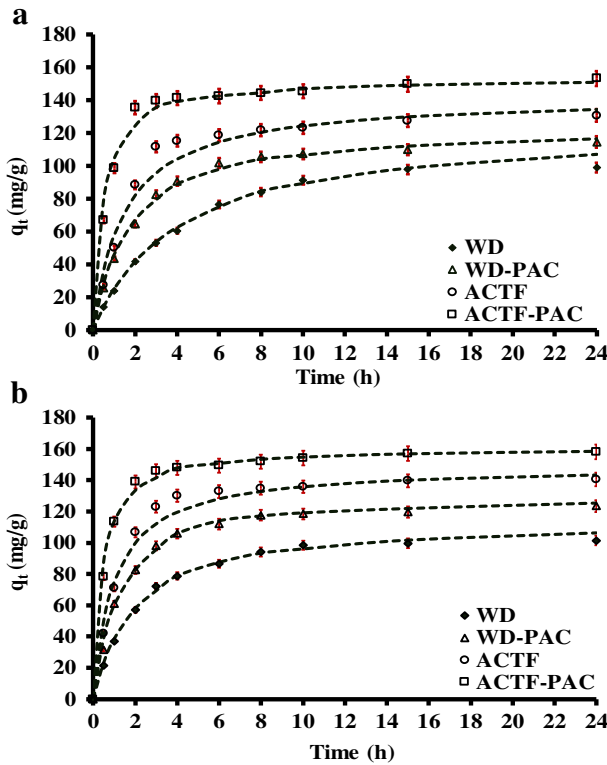


Fig. 4 Effect of contact time on **a** gasoline and **b** condensate oil adsorption by the WD, WD-PAC, ACTF and ACTF-PAC adsorbents (*Symbols* represent experimental data and *dash lines* represent fitted second-order kinetic)

namely Lagergren’s pseudo-first-order, pseudo-second order, Elovich and intraparticle diffusion models (Ho and McKay 1999; Nuithitikul et al. 2010; Lemlikchi et al. 2015; Ferhat et al. 2016; Gupta et al. 2016; Younis and Moustafa 2016) were used to test the experimental oil adsorption data. The kinetics model equations and their outputs constants, as well as their correlation coefficients (R^2) and the error analysis ($\Delta q_t\%$) are tabulated in Table 1. The coefficient R^2 results revealed the high applicability of the second-order kinetic model ($R^2 \approx 1$) to describe the whole adsorption curves of gasoline (Fig. 4a) and condensate (Fig. 4b) oils by the non-modified and PAC-modified WD and ACTF adsorbents over the whole adsorption contact time. On the contrary, inspite of the high Lagergren’s and Elovich kinetic coefficient

Fig. 5 Modification of the adsorbent surfaces with palmitic fatty acid

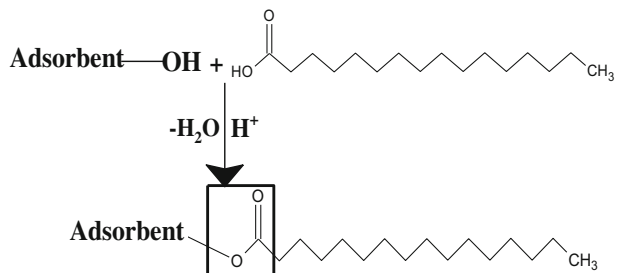


Table 1 The kinetic parameters for adsorption of condensate and gasoline oils by WD, WD-PAC, ACTF and ACTF-PAC adsorbents

Kinetic parameters	WD		WD-PAC		ACTF		ACTF-PAC	
	Condensate	Gasoline	Condensate	Gasoline	Condensate	Gasoline	Condensate	Gasoline
$q_{e,exp}$ (mg.g ⁻¹)	101.46	99.06	123.46	114.54	140.46	130.66	158.08	153.32
Pseudo first-order kinetic model: $\log(q_e - q_t) = \log q_e - \frac{k_1}{2.303}t$								
k_1 (h ⁻¹)	0.27	0.28	0.22	0.21	0.3	0.23	0.26	0.18
$q_{e,calc}$ (mg.g ⁻¹)	76.1	114.54	64.62	71.56	71.7	70.73	46.6	43.92
R^2	0.97	0.96	0.91	0.92	0.95	0.90	0.92	0.81
$\Delta q_t\%$	33.16	11.24	56.03	48.11	54.19	53.37	71.37	73.6
Pseudo second-order kinetic model: $\frac{t}{q_t} = \frac{1}{k_2 q_e^2} + \frac{t}{q_e}$								
k_2 (g.mg ⁻¹ .h ⁻¹)	0.0044	0.002	0.0063	0.0046	0.0067	0.0047	0.015	0.014
$q_{e,calc}$ (mg.g ⁻¹)	114.94	125	131.58	125	149.25	142.86	161.29	153.85
h_0 (mg.g ⁻¹ .h ⁻¹)	57.8	31.35	109.89	72.46	158.73	96.15	384.62	322.58
R^2	0.995	0.997	0.998	0.997	0.999	0.99	0.999	0.999
$\Delta q_t\%$	2.96	2.19	3.97	3.58	5.0	8.5	2.31	4.37
Elovich kinetic model: $q_t = \beta \ln(\alpha\beta) + \beta \ln t$								
α (g.mg ⁻¹ .h ⁻²)	0.21	0.11	0.38	0.22	0.47	0.22	8.73	3.73
β (mg.g ⁻¹ .h ⁻¹)	24.47	26.35	26.08	26.45	28.69	30.38	21.1	22.56
$q_{e,calc}$ (mg.g ⁻¹)	117.6	111	142.45	130.7	166.1	154.72	177.1	171.73
R^2	0.97	0.975	0.94	0.97	0.90	0.91	0.84	0.83
$\Delta q_t\%$	6.39	10.38	10.08	7.07	12.14	14.62	8.29	9.75
Intraparticle diffusion model: $q_t = k_p t^{0.5} + c$								
k_p (mg/g.h ^{0.5})	34.21	32.01	38.54	38.56	53.45	44.91	64.90	58.06
K_{12} (mg.g ⁻¹ .h ^{-0.5})	2.99	4.26	2.78	4.23	3.21	4.32	2.89	4.58
R_1^2	0.95	0.987	0.94	0.952	0.88	0.83	0.92	0.87
R_2^2	0.80	0.79	0.93	0.99	0.92	0.98	0.89	0.99

R^2 results ($R^2 > 0.80$), they do not predict reasonable q_e (mg/g) values. Based on the statistical $\Delta q_t\%$ error in Table 1, the adequacy of fitting kinetic models was ranked in the order of pseudo-second order > Elovich > Lagergren's pseudo-first-order kinetic model, with the lowest $\Delta q_t\%$ error values of 2.31–5.0% and 2.19–8.5% for condensate and gasoline, respectively. This accords with chemisorptions being the rate-controlling of oil adsorption (Sokker et al. 2011; Wang et al. 2016; Younis and Moustafa 2016). In addition, the pseudo-second kinetic assumed that the rate of occupation of binding sites with oil adsorbates is proportional to the square number of the unoccupied active sites on the adsorbent surfaces (Cheu et al. 2016).

In Table 1, q_e and q_t ($\text{mg}\cdot\text{g}^{-1}$) are the amounts of adsorbate adsorbed at equilibrium and time t (h), respectively. K_1 (h^{-1}) and K_2 ($\text{g}\cdot\text{mg}^{-1}\cdot\text{h}^{-1}$) are the pseudo-first and pseudo-second adsorption rate constants. The Elovich constants α and β represent the initial adsorption rate ($\text{g}\cdot\text{mg}^{-1}\cdot\text{h}^{-2}$) and the desorption constant ($\text{mg}\cdot\text{g}^{-1}\cdot\text{h}^{-1}$), respectively. k_i is the intraparticle diffusion constant ($\text{mg}\cdot\text{g}^{-1}\cdot\text{h}^{-0.5}$).

From the oil adsorption curvature results (experimental and theoretical in Fig. 4a and b), two-adsorption stages of linear relationship versus contact time were seen. These findings can suggest that the adsorption of oils by the four adsorbents is not only chemisorption rate-controlling processes, but adsorption may exist in a multilinearity with two adsorption stage mechanisms (Sokker et al. 2011). Thus, the diffusion model was integrated and tested to describe the diffusion mechanism of the adsorption system (Sokker et al. 2011; Younis and Moustafa 2016). Refereing to intraparticle diffusion model (Weber–Morris model), the adsorption mechanism can be divided into three stages ordering, as follows: (1) external mass transfer (exterior sites), (2) capillaries or intraparticle diffusion (internal structure), and (3) adsorption on the internal sorbent surface (interior sites) (Tong et al. 2014). The calculated diffusion rate parameter, k_i ($\text{mg}\cdot\text{g}^{-1}\cdot\text{h}^{-0.5}$) of the intraparticle diffusion (slope of $t^{0.5}$ vs. $q_{t,exp}$; Supplementary data: Fig. S1) and resultant R^2 are listed in Table 1. Obviously, it can be seen that the first stage diffusion rates (k_{i1}) are significantly larger than the second stage (k_{i2}). This is due to the large number of vacant surface sites that are still unoccupied on the adsorbent surface at the beginning, and therefore, a direct fast adsorption arises from the saturation of external surface active sites through film and capillary diffusion mechanisms. With the lapse of time, the adsorption rates decreased due to very low oil residuals in the wastewater solution and high oil adsorbed on the exterior adsorbent surface, which resist the oil diffusion to the remaining intraparticle (capillary and interior) adsorption sites. Nevertheless, both surface and interior adsorption sites take part in the actual adsorption mechanism (Wang et al. 2012; Tong et al. 2014). Hence, adsorption curvatures in Fig. 4 and diffusion rates, k_i , in Table 1 indicate that the oil adsorption capacities are controlled by the second oil equilibrium stages at which intraparticle diffusion mechanism is the rate limit to attain the final adsorption equilibrium state. Analysis of the kinetic rate constants obtained in Table 1 indicate that the oil adsorption was improved by WD-PAC and ACTF-PAC with higher kinetic adsorption rates (K_2) by 1.5 to 3 times, and high affinities for condensate oil adsorption. Furthermore, the obtained diffusion rate, k_i , results in Table 1 suppose that intraparticle diffusion involving the oil diffuses fast into internal adsorbent pores and adsorbent surface active sites ($k_{i1} > k_{i2}$) (Wang et al. 2012; Cheu et al. 2016). Results were confirmed by the high initial adsorption rate (h_o ; $\text{mg}\cdot\text{g}^{-1}\cdot\text{h}^{-1}$) for WD-PAC and ACTF-PAC adsorbents with higher h_o values (72.5–384.6 $\text{mg}\cdot\text{g}^{-1}\cdot\text{h}^{-1}$) compared to WD and ACTF adsorbents (31.35–158.73 $\text{mg}\cdot\text{g}^{-1}\cdot\text{h}^{-1}$).

3.3 Adsorption Isotherm

Adsorption isotherm is critical in design of the practical adsorption system and establishes the appropriate correlation for the adsorption equilibrium curves by the prepared adsorbents (Hamdaoui and Naffrechoux 2007; Younis and Moustafa 2016). In this study, the correlation of isotherm data at C_O of 100–2500 mg oil.L⁻¹ using three nonlinear regression isotherm equations, namely Langmuir, Freundlich and Langmuir-Freundlich models (Younis et al. 2014; Raj and Joy 2015; Ferhat et al. 2016; Younis and Moustafa 2016) were tested to fit the adsorption of condensate and gasoline oils by the fabricated adsorbents.

The three empirical isotherm equations and their corresponding constants, produced by Minitab Statistics (v.17) software, and correlation validity results are shown in Table 2. In Table 2, the magnitude of the Langmuir dimensionless constant of $0.15 \leq R_L < 0.6$ and Freundlich exponent $n > 1$ (n of 1.52–2.50) give an indication of the favorability of both condensate and gasoline oils adsorptions by the prepared adsorbents (Nuithitikul et al. 2010). Under the operating ranges of concentrations studied, the correlation levels between the three isotherm models and experimental data were calculated to be >94% with highest correlation fitting ($R^2 \geq 0.99$, close to unity) by Langmuir-Freundlich model (supplementary data: Figs. S2 and S3). The high correlation fitting of the three isotherm models with experimental isotherm data were confirmed by low $\Delta q_i\% \leq 0.31\%$ (Table 2), suggesting that surface heterogeneity or intraparticle pores on the surfaces of the studied adsorbents played a significant role in oil adsorption (Franz et al. 2000; Schwarz et al. 2004). Comparing the R_L values, it is indicated that the adsorption was more favored by ACTF-PAC (lowest R_L of 0.15) adsorbent than that of other adsorbents, confirming the enhancing of hydrophobicity of ACTF-PAC adsorbent surface. The obtained isotherm results further confirmed that the PAC modified adsorbents (WD-PAC and ACTF-PAC) exhibit improved surface superhydrophobic nature compared to

Table 2 Isotherm parameters for oil adsorption onto WD, WD-PAC, ACTF and ACTF-PAC adsorbents

Isotherm parameters	Condensate oil				Gasoline oil			
	WD	WD-PAC	ACTF	ACTF-PAC	WD	WD-PAC	ACTF	ACTF-PAC
$q_{max,exp}$ (mg.g ⁻¹)	195.00	257.63	304.32	386.86	177.24	225.94	296.11	362.54
Langmuir model ($q_e = \frac{K_L C_e}{1 + a_L C_e}; R_L = \frac{1}{1 + a_L C_e}$)								
$q_{max,calc}$ (mg.g ⁻¹)	227.64	305.00	363.31	447.44	231.64	291.89	354.22	407.98
K_L (L.g ⁻¹)	0.29	0.65	1.70	2.31	0.22	0.62	1.48	2.56
a_L (L.mg ⁻¹)	0.001	0.002	0.005	0.005	0.001	0.002	0.004	0.006
R_L	0.53	0.33	0.18	0.17	0.60	0.33	0.19	0.15
R^2	0.99	0.99	0.99	0.99	0.99	0.99	0.99	0.99
$\Delta q_i\%$	0.05	0.10	0.12	0.12	0.09	0.08	0.15	0.10
Freundlich model $q_e = K_F C_e^{1/n}$								
K_F (L.g ⁻¹)	1.97	5.82	19.06	20.73	1.34	6.54	17.15	24.37
n	1.60	1.88	2.50	2.27	1.52	2.02	2.45	2.47
R^2	0.99	0.97	0.96	0.96	0.99	0.96	0.97	0.94
$\Delta q_i\%$	0.14	0.19	0.22	0.25	0.14	0.21	0.18	0.31
Langmuir-Freundlich model ($q_e = \frac{q_{MLF}(K_{LF}C_e)^{MLF}}{1+(K_{LF}C_e)^{MLF}}$)								
q_{MLF} (mg.g ⁻¹)	230.32	271.31	329.07	404.52	227.49	245.55	317.88	396.49
MLF	1.04	1.07	0.89	0.95	1.01	1.14	0.83	1.01
K_{LF} (L.g ⁻¹)	0.001	0.002	0.004	0.004	0.001	0.002	0.003	0.006
R^2	1.00	0.99	0.99	0.99	0.99	0.99	0.99	0.99
$\Delta q_i\%$	0.04	0.09	0.10	0.11	0.09	0.07	0.10	0.10

the non-modified adsorbents (WD and ACTF). Such improvement of ACTF-PAC organophilic surface properties were confirmed by higher maximum Langmuir–Freundlich q_{MLF} ($\text{mg}\cdot\text{g}^{-1}$) of 271.31 and 245.55 $\text{mg}\cdot\text{g}^{-1}$ and 404.52 and 396.49 $\text{mg}\cdot\text{g}^{-1}$ using WD-PAC and ACTF-PAC compared respectively to q_{MLF} of 230.32 and 227.49 $\text{mg}\cdot\text{g}^{-1}$, and 329.07 and 317.88 $\text{mg}\cdot\text{g}^{-1}$ using WD and ACTF for condensate and gasoline oils.

3.4 Thermodynamic Studies

The temperature effects on the condensate and gasoline oils adsorption by the four adsorbents were evaluated over the temperature range of 288–318 K at C_O of 1000 $\text{mg}\cdot\text{L}^{-1}$. The values of thermodynamic parameters, such as free energy change (ΔG° $\text{kJ}\cdot\text{mol}^{-1}$), standard enthalpy change (ΔH° $\text{kJ}\cdot\text{mol}^{-1}$) and standard entropy changes (ΔS° $\text{kJ}\cdot\text{mol}^{-1}\cdot\text{K}^{-1}$) were calculated from van't Hoff equations (Eq. 5–7) (Younis and Moustafa 2016) and the results are listed in Table S2.

$$\Delta G^\circ = -RT \ln K_c \quad (5)$$

$$\ln K_c = -\frac{\Delta G^\circ}{RT} = \frac{\Delta S^\circ}{R} - \frac{\Delta H^\circ}{RT} \quad (6)$$

$$\Delta G^\circ = \Delta H^\circ - T \Delta S^\circ \quad (7)$$

where R is the ideal gas constant (8.314 $\text{kJ}\cdot\text{mol}^{-1}$), T is the absolute temperature (K), and K_c is the adsorption equilibrium constant.

In this study, the change of a positive sign ΔG° at high temperature (318–313 K) to a negative sign of ΔG° (−1.14 to −0.25 and −1.30 to −0.25 $\text{kJ}\cdot\text{mol}^{-1}$) using ACTF-PAC adsorbent at 288 K and 303 K suggests that the oil adsorption equilibrium shifts to occur in a spontaneous mode at low temperature. In addition, an increase in ΔG° with an increase in temperature indicates a decrease in the feasibility and spontaneity of gasoline and condensate oils adsorption at higher temperatures (Auta and Hameed 2011). The negative values of enthalpy change ($\Delta H^\circ \approx -8.48$ to 21.64 $\text{kJ}\cdot\text{mol}^{-1}$ and −14.18 to 18.33 $\text{kJ}\cdot\text{mol}^{-1}$) imply the exothermic gasoline and condensate oils adsorption character onto the four adsorbents. Smaller values of ΔH° (<40 $\text{kJ}\cdot\text{mol}^{-1}$) are compatible with the formation of weak adsorptive forces between adsorbent and adsorbate. The negative values of ΔS° (< −0.07 $\text{kJ}\cdot\text{mol}^{-1}\cdot\text{K}^{-1}$) suggest that there is a decrease in the randomness at the solid-mixture interface during the adsorption of oil molecules (Bera et al. 2004; Wang et al. 2013).

3.5 Development of Statistical RSM Regression Model Equation

A CCD design was used to develop a mathematical correlation model between the oil adsorption variables and the oil response factor (removal%) by the prepared adsorbents (Demim et al. 2013; Younis and Moustafa 2016). The complete CCD design matrix with the experimental and predicted response values are given in Table S3. It

was found that the actual oil removal percentages were in the ranges 39.5–86.6% and 54.0–98.9% by WD-PAC and ACTF-PAC, respectively, compared to 32.1–60.9% and 39.5–97.2% by WD and ACTF, respectively. According to the sequential model sum of squares (Seq. SS), the quadratic polynomial model was selected as the best-simulated equation representing the experimental results, as suggested by the Design-Expert (v. 8.0.1) software. The four empirical quadratic models in terms of coded variables to simulate the oil removal percentages (Y) by WD, WD-PAC, ACTF and ACTF-PAC adsorbents are presented in Eqs. (8–11), as follows:

$$Y_{WD} = +36.906 + 5.151A + 0.406B - 7.591 \times 10^{-3}C - 0.284A^2 - 9.337 \times 10^{-3}B^2 - 1.277 \times 10^{-6}C^2 - 0.030AB + 8.423 \times 10^{-4}AC + 9.642 \times 10^{-5}BC \tag{8}$$

$$Y_{WD-PAC} = +53.178 + 10.116A - 0.642B - 3.692 \times 10^{-3}C - 0.429A^2 + 5.580 \times 10^{-3}B^2 - 2.323 \times 10^{-6}C^2 - 0.093AB + 3.004 \times 10^{-4}AC + 1.213 \times 10^{-4}BC \tag{9}$$

$$Y_{ACTF} = +33.634 + 11.075A + 1.099B - 8.235 \times 10^{-3}C - 0.347A^2 - 0.022B^2 - 3.121 \times 10^{-6}C^2 - 0.108AB + 4.634 \times 10^{-4}AC + 2.343 \times 10^{-4}BC \tag{10}$$

$$Y_{ACTF-PAC} = +52.932 + 7.133A + 0.961B - 7.729 \times 10^{-3}C - 0.082A^2 - 0.019B^2 - 2.028 \times 10^{-6}C^2 - 0.116AB + 1.121 \times 10^{-4}AC + 2.024 \times 10^{-4}BC \tag{11}$$

The positive and negative sign in front of the model terms indicates synergistic and antagonistic effect on the oil removal responses. The fitting adequacy of the four quadratic regression models in predicting the oil removal was reflected by statistical analysis in Table 3.

The obtained high coefficient value of $R^2 \geq R^2_{Pred} > 0.97$ indicates the adequacy of each model to predict the oil removal responses by their corresponding adsorbent. The adequate precision ratios of 31.39–65.69 indicate an adequate signal, and the simulated model structures (Eqs. 8–11) are reliable and can be used to navigate the oil uptake in the design space (Younis and Moustafa 2016). The actual versus predicted values plots, Fig. S4, further confirm an excellent linear correlation of the selected quadratic model with insignificant standard error deviation (S.D. ≤ 2.3) and lower coefficient of variation ($1.78\% \leq C.V.\% \leq 3.02\%$) for the oil uptake responses. The significance of the model variables was further justified by the ANOVA results listed in Table 4. ANOVA results demonstrate the goodness of the models and significance of the variable combination terms. This is evident from the models F -value of 69.8, 71.3, 275.1 and 61.7 $> F_{Critical}$ (2.49 at $\alpha = 0.05$) with $p \leq 0.0001$ and a lack-of-fit at probability “ p ” < 0.05 for WD, WD-PAC, ACTF and ACTF-PAC adsorbents,

Table 3 Quality of predicted statistical quadratic models based on CCD matrix analysis

Adsorbent	Mean	S. D.	C.V.%	Adequate precision	R^2	R^2_{Pred}
WD	48.83	1.2	2.39	31.39	0.996	0.973
WD-PAC	60.18	1.8	3.02	34.36	0.992	0.974
ACTF	66.61	1.2	1.78	65.69	0.999	0.993
ACTF-PAC	76.51	2.3	2.97	32.07	0.987	0.969

Table 4 ANOVA statistics for the oil adsorption onto WD, WD-PAC, ACTF and ACTF-PAC adsorbents

Source	DF	Seq. SS		F-value				Prob > F "p"-value									
		WD		WD-PAC		ACTF		ACTF-PAC		WD		WD-PAC		ACTF		ACTF-PAC	
		WD	WD-PAC	WD	WD-PAC	WD	WD-PAC	WD	WD-PAC	WD	WD-PAC	WD	WD-PAC	WD	WD-PAC	WD	WD-PAC
Model	9	860.5	2123.7	3498	2869.2	69.8	71.3	275.1	61.7	<0.0001	<0.0001	<0.0001	<0.0001	<0.0001	<0.0001	<0.0001	<0.0001
A	1	391.7	737.2	1544.4	1326.5	285.9	222.7	1092.9	256.8	<0.0001	<0.0001	<0.0001	<0.0001	<0.0001	<0.0001	<0.0001	<0.0001
B	1	73	846.3	522.3	537.4	53.3	255.7	369.6	104	<0.0001	<0.0001	<0.0001	<0.0001	<0.0001	<0.0001	<0.0001	<0.0001
C	1	208.7	303.4	706.4	584.3	152.3	91.7	499.9	113.1	<0.0001	<0.0001	<0.0001	<0.0001	<0.0001	<0.0001	<0.0001	<0.0001
A ²	1	8.5	19.5	12.7	0.7	6.2	5.9	9	0.1	0.0373	0.0414	0.0171	0.721	0.0373	0.0414	0.0171	0.721
B ²	1	12	4.3	69.1	48.8	8.7	1.3	48.9	9.4	0.0183	0.2888	0.0001	0.0153	0.0183	0.2888	0.0001	0.0153
C ²	1	9.2	30.3	54.7	23.1	6.7	9.2	38.7	4.5	0.0323	0.0164	0.0003	0.0674	0.0323	0.0164	0.0003	0.0674
AB	1	10.2	96.6	131.2	152.2	7.5	29.2	92.8	29.5	0.0258	0.0006	<0.0001	0.0006	0.0258	0.0006	<0.0001	0.0006
AC	1	51.1	6.5	15.5	0.9	37.3	1.98	10.9	0.2	0.0003	0.1988	<0.0001	0.6867	0.0003	0.1988	<0.0001	0.6867
BC	1	24.1	38.1	142.3	106.1	17.6	11.5	100.7	20.5	0.003	0.0094	<0.0001	0.0019	0.003	0.0094	<0.0001	0.0019
Residual	8	11	26.5	11.3	41.3												
Lack of Fit	5	10.5	25.9	11	40.7	14.9	27.7	22.3	37.2	0.025	0.0103	0.0141	0.0067	0.025	0.0103	0.0141	0.0067
Pure Error	3	0.4	0.6	0.3	0.7												
Cor Total	17	871.5	2150.2	3509.3	2910.5												

respectively. Thus, ANOVA statistics imply that the proposed four quadratic models (Eqs. 8–11) were of high statistical significance and provide a satisfactory good fit to predict the correlation between the studied variables and oil removal percentages. In this case, linear, interactive and quadratic effects of adsorbent dose, temperature and initial oil concentrations coded as independent factors A, B and C, respectively, are significant model terms. This is reflected by ANOVA data tabulated in Table 4 based on low p -value < 0.05 and high F -value $> F_{Critical}$ of 2.49.

3.6 Response Surface Cube Plots and Optimization of Oil Uptake Operating Conditions

The response cube plot was used to show the interactions and relationships between the adsorbent dose, solution temperature, and initial oil concentrations as independent variables. Figure 6 shows the cube plots of the interactive effects of the three variables on the oil uptake responses over WD, WD-PAC, ACTF, and ACTF-PAC adsorbents. It was clear that all the interaction terms between the three variables have a considerable significant effect on the oil

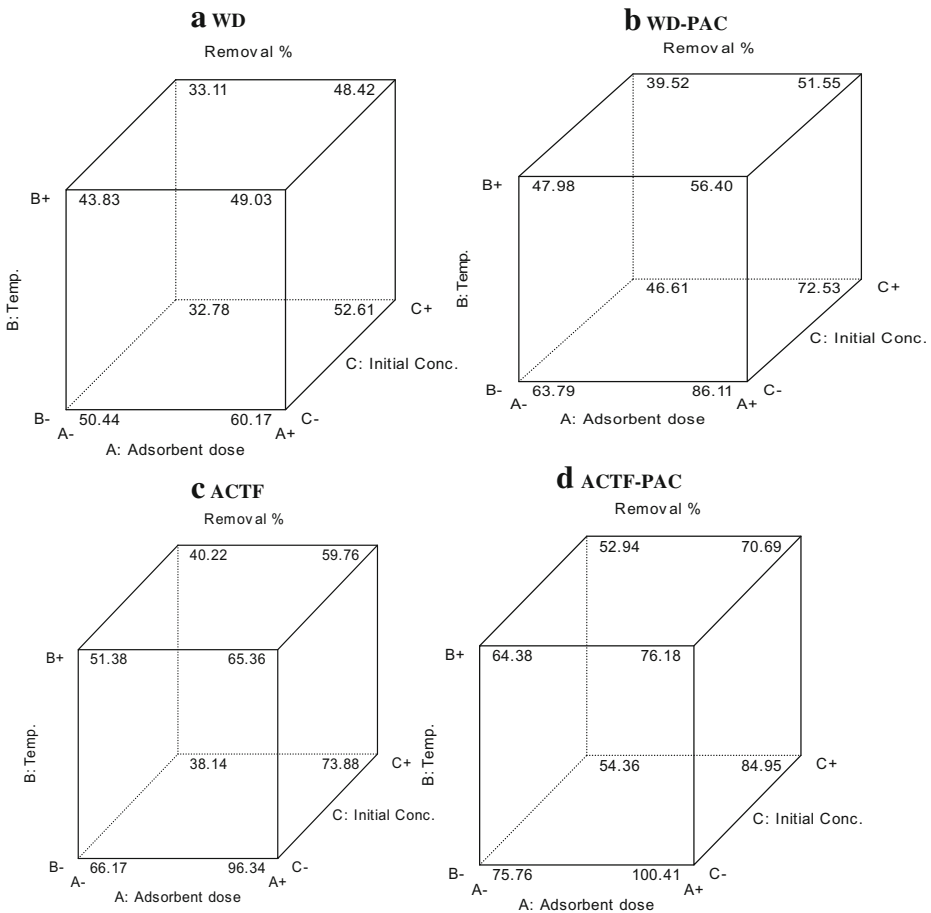


Fig. 6 Response surface cube plots of the interaction effect of adsorbent dose (g/L), temperature (K) and initial oil concentrations (mg/L) on the oil removal efficiency using the prepared adsorbents

adsorption percentage with p level <0.05 (Fig. 6). However, the only A*C interaction term was an insignificant model factor on the oil uptake values (F -value of 1.98 and $0.2 < F_{Critical}$ and p -value of 0.198 and 0.687) when using WD-PAC and ACTF-PAC adsorbents (Table 4). This indicates the improvement of the hydrophobic characteristic of PAC modified adsorbents and the high potential applicability of WD-PAC and ACTF-PAC adsorbents to uptake oils efficiency (Fig. 6b and d) from water solutions, regardless of the initial concentrations of the oil at a large scale. In Fig. 6, a positive relationship can be seen between oil removal response and the adsorbent dose (A), with an inverse relationship with solution temperature (B) and oil concentrations (C) for all the adsorbents. Sharp increase in oil removal is seen with the increase of adsorbent dose (factor A) from 2.5 g.L^{-1} (coded -1) to 7.5 g.L^{-1} (coded $+1$). But, the gradual decrease in oil removal is seen with the increase of solution temperature (factor B) from 288 K (coded -1) to 318 K (coded $+1$) and initial oil concentrations (factor C) from 100 mg.L^{-1} (coded -1) to 2500 mg.L^{-1} (coded $+1$) (Fig. 6). Although the oil removal percentage decreases with increasing oil concentrations, yet the oil adsorbed amount per weight of adsorbent ($q_e, \text{ mg.g}^{-1}$) increases as the initial oil concentration (mg.L^{-1}) increases. By increasing the initial oil concentration from 100 to 2500 mg.L^{-1} , the adsorbed oil per unit weight of adsorbent increased from 8.1 to 176.1 mg.g^{-1} WD, 11.5 to 241 mg.g^{-1} WD-PAC, 13 to 244.5 mg.g^{-1} ACTF, and 13.2 to 283.6 mg.g^{-1} ACTF-PAC at 7.5 g.L^{-1} adsorbent dose and 288 K . The mentioned results were confirmed by the first-order main effect of adsorbent variables on oil removal efficiency through perturbation plots (supplementary data: Fig. S5). Results indicate that the initial oil concentration provides the main driving force to overcome mass-transfer limitations between the oil adsorbates and the prepared adsorbent (Xiaobing et al. 2010; Younis et al. 2014; Zang et al. 2015).

Therefore, an occupation of active binding sites on the adsorbent surface involved in oil adsorption is a fast process at low concentrations. While at higher concentrations, the active binding sites are saturated and further mass-transfer from the liquid to the interior of the solid phase adsorbent is a relatively slow process between the adsorbent and oils adsorbate (Ho and McKay 1999; ShamsiJazeyi et al. 2014; Pan et al. 2016). Thus, the proposed favorable mechanism of adsorption may involve multi-steps as discussed above (cf. Section 3.2.). In this scenario, the oil uptake rate responses by the studied adsorbents can be evaluated with changes in variables using the simulated polynomial model structures. Thus, optimization of adsorption variables are an important stage of the present case to attain a maximum oil uptake from water solutions in case of industrial treatment.

In the present study, the compromises of optimum variable levels were made using the Design Expert software depending upon the highest oil uptake responses as target criteria and model desirability for economic viability. At selected criteria, the desirable variable combination for achieving optimum oils uptake responses by all the four adsorbents was found to be at 6.57 g.L^{-1} adsorbent dose, 308.4 K solution temperature, and 1237.5 mg.L^{-1} initial oil concentration. At these combined conditions, the highest predicted oil adsorption efficiencies were calculated as 53.9 , 63.56 , 76.3 , and 83.9% by WD, WD-PAC, ACTF, and ACTF-PAC, respectively. A validated experimental confirmatory test was found in good harmony with predicted results of experimental oil uptake of 56.4 , 60.9 , 75.2 , and 85.8% by WD, WD-PAC, ACTF, and ACTF-PAC, respectively, under the same optimum conditions. This confirmatory result revealed that the simulated models are effective and reliable for the optimization and prediction of oil uptake behavior by the prepared adsorbents in the industrial application. Furthermore, the PAC treated adsorbents can be used for preventing the oil contaminated wastewater and the dispersion of spilled oil in a shorter time.

3.7 Regeneration and Reusability Study

Another concern about the prepared adsorbents is their regeneration ability for further reuse in remediation of oil contaminated wastewater. A good regeneration ability with an efficient reusability for multiple cycles guarantees that the prepared adsorbent could be economically used for handling oil uptake successively. In this investigation, 2 g of spent PAC modified sorbents (WD-PAC or ACTF-PAC), which have the highest oil adsorption uptake, were collected and repeatedly washed for oil-desorption with 50 mL mixed solution of acetone and ethanol (1:1 vol) at 323 ± 3 K. Then, the efficiency of the oil-desorption was evaluated, while the regenerated sorbents were reused for oil adsorption experiment up to ten cycles. Experimental results in Fig. 7 show that the regenerated WD-PAC and ACTF-PAC kept high oil adsorption performance even after 10 adsorption-desorption cycles. The oil q_e ($\text{mg}\cdot\text{g}^{-1}$) of the recycled adsorbents remained almost unchanged after 5 cycles and a slight gradual decrease by $19.6 \pm 0.59\%$ and $39.2 \pm 0.83\%$ was recorded using WD-PAC and ACTF-PAC, respectively, after ten adsorption cycles (Fig. 7). The mean oil q_e of ten cycles are 313.8 ± 6.89 $\text{mg}\cdot\text{g}^{-1}$ and 188.97 ± 8.13 $\text{mg}\cdot\text{g}^{-1}$ for gasoline (Fig. 7a), and 358.73 ± 7.39 $\text{mg}\cdot\text{g}^{-1}$ and 223.01 ± 7.11 $\text{mg}\cdot\text{g}^{-1}$ for condensate, respectively, using ACTF-PAC and WD-PAC (Fig. 7b). The accumulated q_e of one gram of PAC modified adsorbents, assuming that the adsorbents are reused ten times successively, can be calculated respectively to be 1889.7 to 3138.4 mg gasoline oil and 2230.5 to 3587.3 mg condensate oil using WD-PAC and ACTF-PAC. The successive high oil adsorption can be explained by the stability of PAC functionalities on the WD and ACTF surfaces, and this suggests an extraordinary reusability of the adsorbent

Fig. 7 Desorption-adsorption cycles of the WD-PAC and ACTF-PAC adsorbents for adsorption of **a** gasoline oil, and **b** condensate oil from wastewater at optimum operating conditions

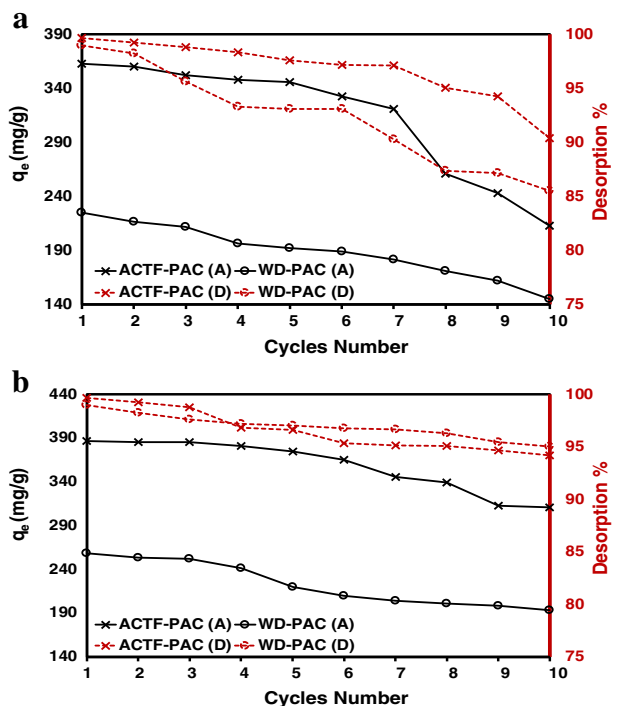


Table 5 Oil adsorption capacities (gram oil per gram sorbent) compared with some reported adsorbents in literature

Adsorbents	C_o (g.L ⁻¹)	Adsorption capacity (q_e , g.g ⁻¹)	References
Chitosan based 40% polyacrylamide (PAM) hydrogel	30.0	1.80	(Sokker et al. 2011)
lignite activated coke (LAC) ^a	---	0.573	(Tong et al. 2014)
Surfactant modified barley straw (SMBS)	3.45	0.576	(Ibrahim et al. 2010)
Bentonite	1.613	0.552	(Okiel et al. 2011)
Powder activated carbon (PAC)	1.613	0.468	
Deposited carbon (DC)	1.613	0.570	
Bentonite organoclay	0.38	0.14	(Moazed and Viraraghavan 2005)
Expanded vermiculite	0.005–0.502 ^b	$8.1 \times 10^{-3} - 4.6 \times 10^{-2}$ ^b	(Mysore et al. 2005)
Hydrophobized vermiculite	0.005–0.502 ^b	$2.7 \times 10^{-3} - 2.3 \times 10^{-2}$ ^b	
Walnut shell adsorbent	---	0.56–0.74 ^b	(Srinivasan and Viraraghavan 2008)
Treated yellow horn shell residues by ionic liquid (IL)	100.0	0.46–0.71 ^b	(Li et al. 2013)
M-NBS-PAL sorbent	5.0	1.70	(Cheu et al. 2016)
M-NBS-PAL sorbent	0.3	0.091	(Cheu et al. 2016)
WD-PAC	2.5	0.23–0.26 ^b	This study
ACTF-PAC	2.5	0.36–0.39 ^b	This study

^a Heavy oil removal capacity determined by chemical oxygen demand (COD)

^b Adsorption capacity is oil type dependent

materials. Indeed, contrary to high condensate oil uptake and desorption efficiency over 95% (Fig. 7b), the gasoline desorption efficiency gradually decreased after the 6 cycles to reach 90.4 and 85.6% for ACTF-PAC and WD-PAC, respectively, at the run number ten (Fig. 7a). This may be attributed to the capillary and interior pores adsorbent saturation, which implies that at this stage more time could be needed for gasoline oil-desorption from the interior surface sites. With the decrease of oil regeneration from adsorbents, the unoccupied active sites consequently decrease, causing less oil to be adsorbed by the used WD-PAC and ACTF-PAC (Fig. 7).

Table 5 presents a comparison of the uptake efficiencies in terms of maximum q_e (g.g⁻¹) of the WD-PAC and ACTF-PAC as potential adsorbents for treatment of oil contaminated wastewater in this study with previously literature adsorbents. Obviously, the WD-PAC and ACTF-PAC gave a high or approximate similar q_e (g.g⁻¹) compared to almost all referenced adsorbents. Compared to other adsorbents, the chitosan based 40% polyacrylamide (PAM) hydrogel and M-NBS-PAL adsorbents (Sokker et al. 2011; Cheu et al. 2016) exhibit much higher q_e (g.g⁻¹) by three to four times than the prepared adsorbents in this study. Taking the initial oil concentration as the point of reference, this greater q_e may be due to the additional treatment of these adsorbents beside the high initial oil concentration used which is higher by 2–12 times than the maximum oil concentration used in this study. In general, based on the experimental and calculated results it can be concluded that, it could be of great economic significance to use the prepared adsorbents to treat and/or prevent oil pollution in industrial case as it will only

require less than 0.448 to 0.278 tons sorbents to clean one ton of spilled oil depending on oil contamination sources.

4 Conclusions

To sum up, in this article a simple approach to develop superhydrophobic amorphous carbon thin film (ACTF) fabricated from wood sawdust (WD) through surface functionalization with palmitic acids (PAC – C₁₆) is investigated to adsorb condensate and gasoline oils from wastewater solutions. The relevant adsorption results showed that the oils uptake kinetics were found to be adequately fitted to pseudo-second order > Elovich > Lagergren's pseudo-first-order kinetic model as validated by the highest $R^2 \geq 0.99$ and lowest statistical $\Delta q, \%$ errors $\leq 8.5\%$. Regarding the isotherm theories, the three-parameter Langmuir-Freundlich gave the best fit to the experimental q_e (mg.g⁻¹) of gasoline and condensate oils compared to the simulation exhibited by the two-parameter Langmuir and Freundlich models. The thermodynamic study demonstrated the exothermic nature of oil adsorption by the four adsorbents with an inverse q_e (mg.g⁻¹) correlation with temperature. Based on ANOVA results of CCD experimental adsorption matrix, four empirical quadratic models were developed to simulate the relationship between adsorption variables and oils uptake responses with high adequacy at p-value <0.05 and coefficient values of $R^2 \geq R^2_{Pred} > 0.97$. The response surface cube plots of oil responses revealed that the interaction effects of adsorbent dose and initial oil concentrations have insignificant effect on the oil removal efficiencies by WD-PAC and ACTF-PAC (F-value of 1.98 and $0.2 < F_{Critical}$ and p-value of 0.198 and 0.687). This is because of the improvement of the hydrophobic characteristic by PAC functionalities, which facilitate hydrophobic and partition mechanism with organophilic oil components in the wastewater environment. This is confirmed by higher oil uptake rate (h_o) of PAC-C₁₆ modified adsorbents by 2–2.5 times compared to nonmodified WD and ACTF adsorbents with improved oil uptake rates in the order of WD < WD-PAC < ACTF < ACTF-PAC. Moreover, the WD-PAC and ACTF-PAC adsorbents proved to be efficient, renewable and reusable potential candidates to treat and/or prevent oil contamination with the assumed accumulated q_e of 1889.7 to 3138.4 mg.g⁻¹ for gasoline oil, and 2230.5 to 3587.3 mg.g⁻¹ for condensate oil using WD-PAC and ACTF-PAC after ten cycles. In conclusion, the results obtained suggest the application potential of the low-cost superhydrophobic WD-PAC and ACTF-PAC adsorbents for uptaking dissolved or spilled oil from wastewater efficiently, regardless of the initial oil concentrations.

References

- Auta M, Hameed BH (2011) Preparation of waste tea activated carbon using potassium acetate as an activating agent for adsorption of acid blue 25 dye. Chem Eng J 171:502–509
- Banerjee SS, Joshi MV, Jayaram RV (2006) Treatment of oil spill by sorption technique using fatty acid grafted sawdust. Chemosphere 64:1026–1031
- Bera D, Lahiri D, Nag A (2004) Kinetic studies on bleaching of edible oil using charred sawdust as a new adsorbent. J Food Eng 65:33–36
- Cambiella A, Ortea E, Rios G et al (2006) Treatment of oil-in-water emulsions: performance of a sawdust bed filter. J Hazard Mater 131:195–199
- Chen C, Wei L, Guo X et al (2014) Investigation of heavy oil refinery wastewater treatment by integrated ozone and activated carbon-supported manganese oxides. Fuel Process Technol 124:165–173

- Cheu SC, Kong H, Song ST et al (2016) Separation of dissolved oil from aqueous solution by sorption onto acetylated lignocellulosic biomass - equilibrium, kinetics and mechanism studies. *J Environ Chem Eng* 4: 864–881. doi:10.1016/j.jece.2015.12.028
- Demim S, Drouiche N, Aouabed A, Semsari S (2013) CCD study on the ecophysiological effects of heavy metals on *Lemna gibba*. *Ecol Eng* 57:302–313
- Dong Z, Lu M, Huang W, Xu X (2011) Treatment of oilfield wastewater in moving bed biofilm reactors using a novel suspended ceramic biocarrier. *J Hazard Mater* 196:123–130
- El-Sayed M, Ramzi M, Hosny R et al (2016) Breakthrough curves of oil adsorption on novel amorphous carbon thin film. *Water Sci Technol* 73:2361–2369. doi:10.2166/wst.2016.072
- Fard AK, Rhadfi T, Mckay G et al (2016) Enhancing oil removal from water using ferric oxide nanoparticles doped carbon nanotubes adsorbents. *Chem Eng J* 293:90–101
- Ferhat M, Kadouche S, Drouiche N et al (2016) Competitive adsorption of toxic metals on bentonite and use of chitosan as flocculent coagulant to speed up the settling of generated clay suspensions. *Chemosphere* 165:87–93
- Franz M, Arafat HA, Pinto NG (2000) Effect of chemical surface heterogeneity on the adsorption mechanism of dissolved aromatics on activated carbon. *Carbon* 38:1807–1819. doi:10.1016/S0008-6223(00)00012-9
- Ge B, Zhang Z, Zhu X et al (2014) A superhydrophobic/superoleophilic sponge for the selective absorption of oil pollutants from water. *Colloids Surf A Physicochem Eng Asp* 457:397–401
- Gupta S, He W-D, Tai N-H (2016) A comparative study on superhydrophobic sponges and their application as fluid channel for continuous separation of oils and organic solvents from water. *Compos Part B Eng* 101:99–106
- Hamdaoui O, Naffrechoux E (2007) Modeling of adsorption isotherms of phenol and chlorophenols onto granular activated carbon: part II. Models with more than two parameters. *J Hazard Mater* 147:401–411
- Hameed BH (2007) Equilibrium and kinetics studies of 2, 4, 6-trichlorophenol adsorption onto activated clay. *Colloids Surf A Physicochem Eng Asp* 307:45–52
- Hartmann J, Beyer R, Harm S (2014) Effective removal of estrogens from drinking water and wastewater by adsorption technology. *Environ Process* 1:87–94. doi:10.1007/s40710-014-0005-y
- Heibati B, Rodriguez-Couto S, Al-Ghouti MA et al (2015) Kinetics and thermodynamics of enhanced adsorption of the dye AR 18 using activated carbons prepared from walnut and poplar woods. *J Mol Liq* 208:99–105
- Ho Y-S, McKay G (1999) Pseudo-second order model for sorption processes. *Process Biochem* 34:451–465
- Hosny R, Fathy M, Ramzi M et al (2016) Treatment of the oily produced water (OPW) using coagulant mixtures. *Egypt J Pet* 25:391–396. doi:10.1016/j.ejpe.2015.09.006
- Ibrahim S, Wang S, Ang HM (2010) Removal of emulsified oil from oily wastewater using agricultural waste barley straw. *Biochem Eng J* 49:78–83
- Jain CK, Malik DS (2016) Applicability of plant based biosorbents in the removal of heavy metals : a review. *Environ Process* 3:495–523. doi:10.1007/s40710-016-0143-5
- Lemlikich W, Drouiche N, Belaicha N et al (2015) Kinetic study of the adsorption of textile dyes on synthetic hydroxyapatite in aqueous solution. *J Ind Eng Chem* 32:233–237
- Li J, Luo M, Zhao CJ, Li CY, Wang W, Zu YG, Fu YJ (2013) Oil removal from water with yellow horn shell residues treated by ionic liquid. *Bioresour Technol* 128:673–678. doi:10.1016/j.biortech.2012.11.009
- Majdan M, Maryuk O, Pikus S et al (2005) Equilibrium, FTIR, scanning electron microscopy and small wide angle X-ray scattering studies of chromates adsorption on modified bentonite. *J Mol Struct* 740:203–211
- Malik R, Mukherjee M, Swami A et al (2004) Validation of adsorption efficiency of activated carbons through surface morphological characterization using scanning electron microscopy technique. *Carbon Lett* 5:75–80
- Meniai AH (2012) The use of sawdust as by product adsorbent of organic pollutant from wastewater: adsorption of phenol. *Energy Procedia* 18:905–914
- Moazed H, Viraraghavan T (2005) Removal of oil from water by bentonite organoclay. *Pract Period Hazardous, Toxic, Radioact Waste Manag* 9:130–134. doi:10.1061/(ASCE)1090-025X(2005)
- Munthali MW, Johan E, Aono H, Matsue N (2015) Cs⁺ and Sr²⁺ adsorption selectivity of zeolites in relation to radioactive decontamination. *Integr Med Res* 3:245–250
- Mysore D, Viraraghavan T, Jin Y (2005) Treatment of oily waters using vermiculite. *Water Res* 39:2643–2653. doi:10.1016/j.watres.2005.04.034
- Nuithitikul K, Srihoun S, Hirunpraditkoon S (2010) Kinetics and equilibrium adsorption of Basic Green 4 dye on activated carbon derived from durian peel: effects of pyrolysis and post-treatment conditions. *J Taiwan Inst Chem Eng* 41:591–598
- Okiel K, El-Sayed M, El-Kady MY (2011) Treatment of oil–water emulsions by adsorption onto activated carbon, bentonite and deposited carbon. *Egypt J Pet* 20:9–15
- Pan Y, Wang J, Sun C et al (2016) Fabrication of highly hydrophobic organic–inorganic hybrid magnetic polysulfone microcapsules: a lab-scale feasibility study for removal of oil and organic dyes from environmental aqueous samples. *J Hazard Mater* 309:65–76
- Pandey KK, Pitman AJ (2003) FTIR studies of the changes in wood chemistry following decay by brown-rot and white-rot fungi. *Int Biodeterior Biodegrad* 52:151–160

- Patai S (1966) The chemistry of the carbonyl group (volume 1). Interscience, London, New York, Sydney
- Raj KG, Joy PA (2015) Coconut shell based activated carbon–iron oxide magnetic nanocomposite for fast and efficient removal of oil spills. *J Environ Chem Eng* 3:2068–2075
- Roberts CM, Inniss EC (2014) Implementing treatment sequences to promote reduction of DBPs in small drinking water systems. *Water Resour Manag* 28:1631–1643. doi:10.1007/s11269-014-0570-x
- Roustaei A, Saffarzadeh S, Mohammadi M (2013) An evaluation of modified silica nanoparticles' efficiency in enhancing oil recovery of light and intermediate oil reservoirs. *Egypt J Pet* 22:427–433
- Sayed SA, Zayed AM (2006) Investigation of the effectiveness of some adsorbent materials in oil spill clean-ups. *Desalination* 194:90–100. doi:10.1016/j.desal.2005.10.027
- Schwarz JA, Contescu CI, Putyera K (2004) Dekker encyclopedia of nanoscience and nanotechnology. CRC press, Marcel Dekker, Inc., New York, p 24. doi:10.1081/E-ENN 120013563
- ShamsiJazeyi H, Verduzco R, Hirasaki GJ (2014) Reducing adsorption of anionic surfactant for enhanced oil recovery: part I. Competitive adsorption mechanism. *Colloids Surf A Physicochem Eng Asp* 453:162–167. doi:10.1016/j.colsurfa.2013.10.042
- Sidik SM, Jalil AA, Triwahyono S et al (2012) Modified oil palm leaves adsorbent with enhanced hydrophobicity for crude oil removal. *Chem Eng J* 203:9–18
- Smith MB, March J (2007) March's advanced organic chemistry: reactions, mechanisms, and structure. Wiley
- Sokker HH, El-Sawy NM, Hassan MA, El-Anadouli BE (2011) Adsorption of crude oil from aqueous solution by hydrogel of chitosan based polyacrylamide prepared by radiation induced graft polymerization. *J Hazard Mater* 190:359–365. doi:10.1016/j.jhazmat.2011.03.055
- Srinivasan A, Viraraghavan T (2008) Removal of oil by walnut shell media. *Bioresour Technol* 99:8217–8220. doi:10.1016/j.biortech.2008.03.072
- Tong K, Zhang Y, Fu D et al (2014) Removal of organic pollutants from super heavy oil wastewater by lignite activated coke. *Colloids Surf A Physicochem Eng Asp* 447:120–130. doi:10.1016/j.colsurfa.2014.01.062
- Wang B, Zhou K, Liu H (2016) Biosorption behavior and reuse potential of waste biomass of *Aspergillus fumigatus*, previously used in humic acid biosorption, in removal of reactive blue 49. *Environ Process* 3(4): 843–856. doi:10.1007/s40710-016-0188-5
- Wang D, McLaughlin E, Pfeffer R, Lin YS (2012) Adsorption of oils from pure liquid and oil – water emulsion on hydrophobic silica aerogels. *Sep Purif Technol* 99:28–35
- Wang J, Zheng Y, Wang A (2013) Coated kapok fiber for removal of spilled oil. *Mar Pollut Bull* 69:91–96
- Wu J, Wang N, Wang L et al (2012) Electrospun porous structure fibrous film with high oil adsorption capacity. *ACS Appl Mater Interfaces* 4:3207–3212
- Xiaobing LI, ZHANG C, Jiongtian LIU (2010) Adsorption of oil from waste water by coal: characteristics and mechanism. *Min Sci Technol* 20(7):78–781
- Yang H, Yan R, Chen H et al (2007) Characteristics of hemicellulose, cellulose and lignin pyrolysis. *Fuel* 86: 1781–1788
- Yang M (2011) Measurement of oil in produced water. In: Produced water. Springer, pp 57–88
- Younis SA, El-Gendy NS, El-Azab WI et al (2014) The Biosorption of phenol from petroleum refinery wastewater using spent waste biomass. *Energy Sources, Part A Recover Util Environ Eff* 36:2566–2578
- Younis SA, Moustafa YM (2016) Synthesis of urea-modified MnFe₂O₄ for aromatic micro- pollutants adsorption from wastewater: mechanism and modeling. *Clean Techn Environ Policy*. doi:10.1007/s10098-016-1244-6
- Zang D, Liu F, Zhang M, Niu XG, Gao ZX, Wang CY (2015) Superhydrophobic coating on fiberglass cloth for selective removal of oil from water. *Chem Eng J* 262:210–216